

1 Leveraging genetic ancestry continuum information 2 to interpolate PRS for admixed populations

3
4 Yunfeng Ruan¹, Rohan Bhukar^{1,2}, Aniruddh Patel^{1,2,3}, Satoshi Koyama^{1,2,3,4}, Leland
5 Hull^{5,6}, Buu Truong^{1,2,3,8}, Whitney Hornsby^{1,2}, Haoyu Zhang⁷, Nilanjan Chatterjee^{9,10},
6 Pradeep Natarajan^{1,2,3,6}

7 Affiliations:

- 8 1. Program in Medical and Population, Genetics and Cardiovascular Disease
9 Initiative, Broad Institute of Harvard and MIT, Cambridge, MA, USA
- 10 2. Cardiovascular Research Center, Massachusetts General Hospital, Boston,
11 MA, USA
- 12 3. Center for Genomic Medicine, Massachusetts General Hospital, Boston, MA,
13 USA, USA
- 14 4. Laboratory for Cardiovascular Genomics and Informatics, RIKEN Center for
15 Integrative Medical Sciences, Yokohama, Japan
- 16 5. Division of General Internal Medicine, Massachusetts General Hospital,
17 Boston, MA, USA
- 18 6. Department of Medicine, Harvard Medical School, Boston, MA, USA
- 19 7. Division of Cancer Epidemiology and Genetics, National Cancer Institute,
20 Bethesda, MD, USA
- 21 8. Department of Genetic Epidemiology and Statistical Genetics, Harvard
22 T.H. School of Public Health, Cambridge, MA, US
- 23 9. Department of Biostatistics, Bloomberg School of Public Health, Johns
24 Hopkins University, Baltimore, MD, USA
- 25 10. Department of Oncology, School of Medicine, Johns Hopkins University,
26 Baltimore, MD, USA

27
28
29 Please address correspondence to:

30 Pradeep Natarajan, MD MMSc
31 185 Cambridge Street, CPZN 5.238
32 Boston, MA 02446
33 617-726-1843
34 pnatarajan@mg.harvard.edu

35 Funding:

36 P.N. is supported by NHGRI U01HG011719 and NHLBI R01HL127564. N.C is
37 supported by NHGRI U01HG011719 and R01HG010480. A.P.P. is supported by
38 NHLBI K08HL168238.
39

40 Disclosures:

41 P.N. reports research grants from Allelica, Amgen, Apple, Boston Scientific,
42 Genentech / Roche, and Novartis, personal fees from Allelica, Apple, AstraZeneca,
43 Blackstone Life Sciences, Bristol Myers Squibb, Creative Education Concepts,
44 CRISPR Therapeutics, Eli Lilly & Co, Esperion Therapeutics, Foresite Capital,
45 Foresite Labs, Genentech / Roche, GV, HeartFlow, Magnet Biomedicine, Merck,
46 Novartis, Novo Nordisk, TenSixteen Bio, and Tourmaline Bio, equity in Bolt, Candela,
47 Mercury, MyOme, Parameter Health, Preciseli, and TenSixteen Bio, and spousal
48 employment at Vertex Pharmaceuticals, all unrelated to the present work. All other
49
50

51 authors report no conflicts.

52 Abstract

53 The relatively low representation of admixed populations in both discovery and fine-
54 tuning individual-level datasets limits polygenic risk score (PRS) development and
55 equitable clinical translation for admixed populations. Under the assumption that the
56 most informative PRS weight for a homogeneous sample varies linearly in an
57 ancestry continuum space, we introduce a Genetic **Distance**-assisted PRS
58 **Combination Pipeline for Diverse Genetic Ancestries (DiscoDivas)** to interpolate a
59 harmonized PRS for diverse, especially admixed, ancestries, leveraging multiple
60 PRS weights fine-tuned within single-ancestry samples and genetic distance.
61 DiscoDivas treats ancestry as a continuous variable and does not require shifting
62 between different models when calculating PRS for different ancestries. We
63 generated PRS with DiscoDivas and the current conventional method, i.e. fine-tuning
64 multiple GWAS PRS using the matched or similar ancestry samples. DiscoDivas
65 generated a harmonized PRS of the accuracy comparable to or higher than the
66 conventional approach, with the greatest advantage exhibited in admixed individuals.
67

68 Introduction/Main

69 Individuals who are not of European ancestry remain underrepresented in genome-
70 wide association studies (GWAS), which at least partly explains why polygenic risk
71 score (PRS) performance is generally reduced in this population when compared
72 with individuals of European ancestry¹. Within the constraints of existing data, the
73 current principal solution to increase the PRS accuracy among non-European
74 individuals is to fine-tune a combination of PRS derived from multiple populations or
75 multiple traits with the individual-level data of a training cohort²⁻⁶. However, PRS
76 accuracy decays as the genetic distance between the fine-tuning and testing
77 samples increases⁷. Relative to the vast diversity across the genetic ancestry
78 continuum, the existing and near-term individual-level datasets that can be used for
79 fine-tuning PRS combinations remains very sparse. Most existing individual-level
80 genotype data are mainly collected from single-ancestry populations and therefore
81 admixed populations are left underrepresented or are largely excluded from analysis
82 ⁸⁻¹¹. Additionally, fine-tuning and testing samples that are labeled as “from the same
83 superpopulation” are often truly genetically heterogeneous^{10,12-15}, leading to variable
84 accuracy within such samples.

85
86 PRS analysis across diverse ancestries may also be limited by inconsistency. The
87 raw PRS distributions of the same model varies by ancestry and therefore the raw
88 PRS values for individuals of different genetic ancestries should not be directly
89 compared without ancestry correction¹⁶⁻¹⁸. Although prior research^{16,18,19} has shown
90 that regressing out the top principal components of ancestry (PCA) from the PRS can
91 unify the PRS distributions of different ancestries (i.e., the mean and standard
92 deviation of corrected PRS sampled from different populations can become very
93 close), the inconsistency is only partially solved. In the application of PRS across
94 diverse ancestries, one would have to use one PRS model for all the individuals,
95 causing inconsistent PRS accuracy, or use several discrete PRS models for different
96 individuals approximating superpopulations also causing inconsistent PRS modelling
97 and accuracy.

98

99 Given these issues and the increasing clinical use of PRS^{20–22}, PRS generation for
100 diverse and admixed genetic ancestries with more consistent accuracy and more
101 unified PRS distributions is critically needed. We devised a method, DiscoDivas, a
102 Genetic **D**istance-assisted PRS **C**ombination Pipeline for **D**iverse Genetic
103 **A**ncestries, to generate PRS across the genetic ancestry continuum. This method is
104 based on the recent observation⁷ that the PRS accuracy in the testing data decays
105 approximately linearly as the genetic distance between the fine-tuning and samples
106 increases, and that the genetic distance can be approximated by Euclidian distance
107 of PCA based on the global ancestries⁷. Based on this observation, we assumed that
108 the most informative PRS weights for a sample can be linearly interpolated from the
109 currently available PRS weights that are fine-tuned in the ancestries surrounding it in
110 the global ancestry-based PCA space with the interpolation weights based on the
111 Euclidian distance of the PCA. In summary, DiscoDivas calculates PRS for diverse
112 and admixed genetic ancestries whose genetic data may not be sufficiently powerful
113 alone to train a PRS model by linearly interpolating the multiple PRS fine-tuned in
114 ancestries whose genetic data are more available. We evaluated its performance in
115 simulated and empiric data.
116

117 Results

118 Overview of DiscoDivas

119 DiscoDivas combines PRS fine-tuned in different fine-tuning samples - generally from
120 different single-ancestry populations - to linearly interpolate PRS for individuals of
121 diverse genetic ancestries, treating ancestry as a continuous variable. The rationale
122 for PRS combination is based on the observation that the correlation of the most
123 informative PRS weight for two samples of different ancestry drops as the genetic
124 distance, represented by Euclidean distance of global ancestry-based PCA,
125 increases⁷. Therefore, the best PRS weight for an ancestry representation can be
126 linearly interpolated from other PRS weights fine-tuned in other ancestries with the
127 additional consideration of the genetic distance between the samples (Figure 1).
128

129 Under the same principle of interpolating the PRS weight, the best PRS can be
130 interpolated from several PRS calculated using the weight fine-tuned in other
131 ancestries. Since generating individual-specific PRS weights in a testing dataset
132 causes redundant calculation and given the difficulty of normalizing information from
133 different datasets, we combine the PRS instead of the SNP weights. The PRS of
134 individuals in the testing sample is a linear combination of PRS based on the SNP
135 weights fine-tuned in different fine-tuning samples:

$$136 \quad PRS_i = \sum w_{i,k} PRS_{i,k}$$

137 where $PRS_{i,k}$ is the PRS of testing individual i calculated using the weight fine-tuned
138 in the fine-tuning sample k ; $w_{i,k}$ is the combination coefficient mainly based on the
139 reciprocal of the PCA Euclidean distance between the testing individual and median
140 point of the fine-tuning sample $D_{i,k}$. Note that the input PRS and PCA should be of
141 the same scale: all the individuals are projected to the same PCA space based on a
142 global ancestry reference panel and the PRS input $PRS_{i,k}$ is the raw PRS regressed
143 out the top PCs and then standardized. Additionally, we recommend including all
144 available discovery GWAS for PRS in each PRS model fine-tuned in the single-

145 ancestry sample to maximize the PRS accuracy, as indicated in Figure 1.
146 Nevertheless, DiscoDivas is a flexible framework that allows the different sets of
147 discovery GWAS and fine-tuning method used in different fine-tuning samples.

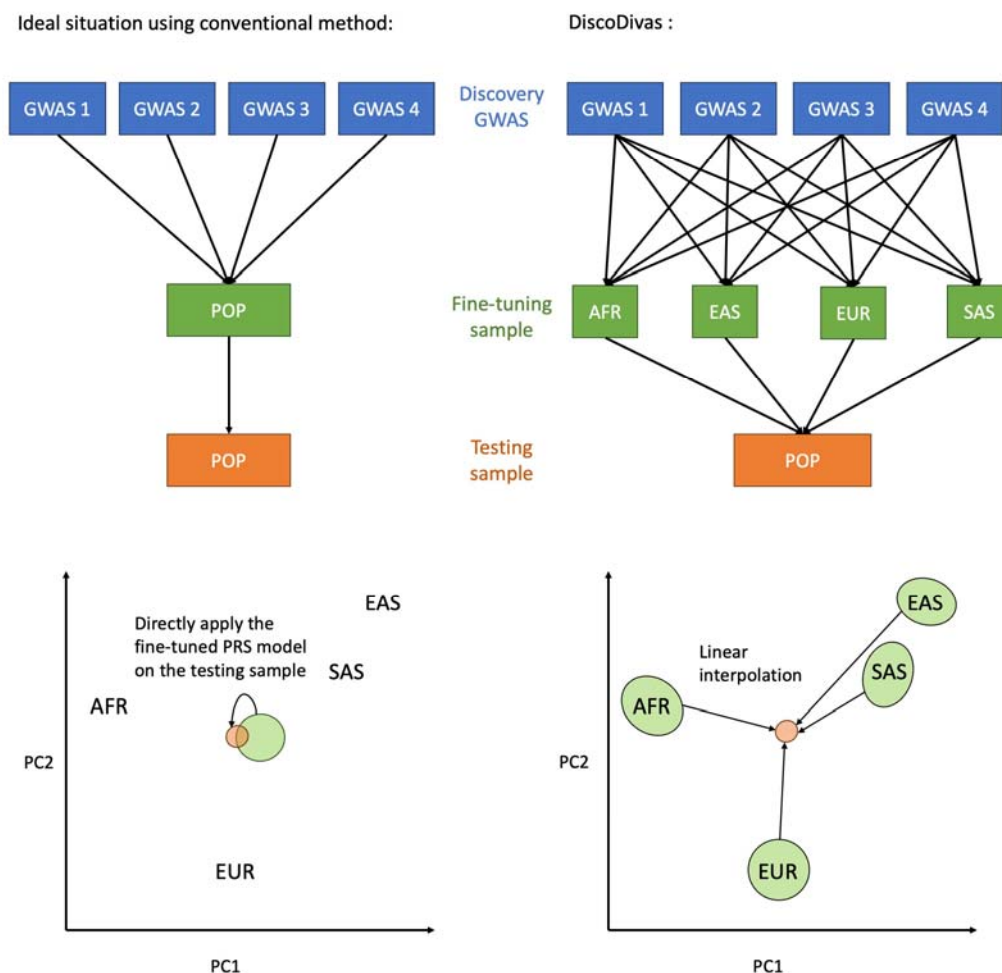
148
149 In addition to the PCA distances, other factors are included in the model. First, since
150 some fine-tuning samples are more correlated than others (e.g., EAS and SAS are
151 more correlated than AFR and EUR), the combination coefficients should be further
152 modified by these correlations, which can also be extracted from the PCA Euclidean
153 distances. Second, since PRS fine-tuned in each of the fine-tuning samples may be
154 of differing qualities (e.g., when the PRS model fine-tuned in different samples are
155 based on GWAS of different sample sizes or populations), the quality of the PRS
156 trained with each of the training data will vary and should be taken into account when
157 combining the PRS. Thus, the combination coefficient $w_{i,k}$ in the previous formula is
158 a function of multiple factors:

$$w_{i,k} = f\left(\frac{1}{D_{i,k}}, G, r_k\right)$$

159 where $\frac{1}{D_{i,k}}$ is the reciprocal of PCA Euclidean distance between the individual i and
160 the fine-tuning sample k ; G is the matrix of PCA Euclidean distance between fine-
161 tuning samples; r_k is the parameter describing the quality of training fine-tuning
162 samples. A more detailed description of defining $w_{i,k}$ is given in the supplementary
163 method section entitled 'Methodological Details of DiscoDivas'.

164
165 The PRS input for DiscoDivas in this study was the multi-GWAS PRS fine-tuned in
166 AFR, EAS, EUR, and SAS fine-tuning samples with the conventional method pipeline
167 as mentioned above (see the following section titled "Overview of multi-population
168 GWAS PRS model" for more detailed information of the input PRS). The interpolation
169 of these four PRS is based on the PCA calculated using the 1000 Genomes
170 reference panel. For most of the PRS analysis conducted in in the present study, the
171 input PRS of DiscoDivas are based on the same set of discovery GWAS and the
172 fine-tuning datasets are sufficiently large to generate a stable result. Therefore, we
173 assumed that all the input PRS can be viewed as of equal quality and their parameter
174 for PRS quality r_k can be viewed as a constant value in the present study.

175 Overview of multi-population GWAS PRS model



176
 177 **Figure 1: The workflow of comparing DiscoDivas with the existing method.** Left: The ideal situation
 178 for the existing method is to fine-tune a PRS model that contains multiple GWAS with matched fine-
 179 tuning data, which is not currently available for many under-represented populations. Right: DiscoDivas
 180 first fine-tunes the PRS in the available ancestries, which are currently AFR, EAS, EUR, and SAS, and
 181 interpolates PRS for diverse ancestry groups based on these fine-tuned PRS. In this plot, POP refers to
 182 any ancestry for which the PRS is to be calculated.

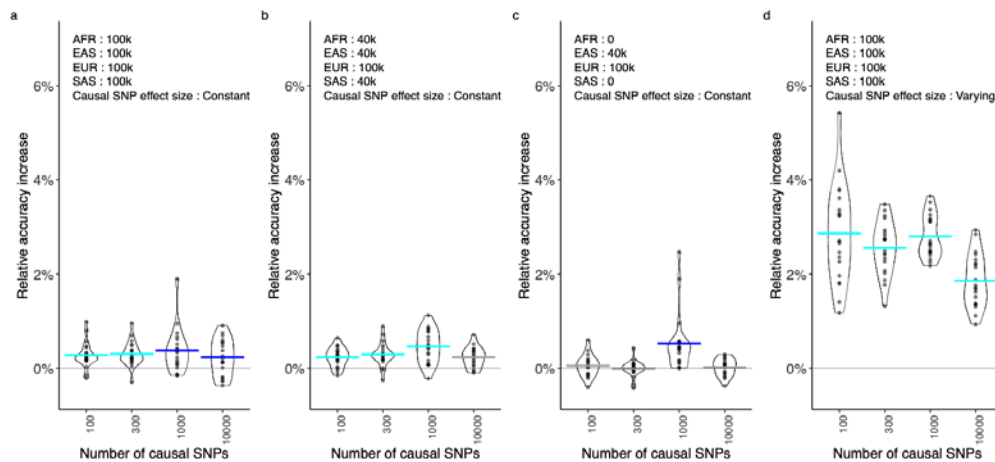
183
 184 A common approach for constructing PRS is to include as much genome-wide
 185 association study (GWAS) summary statistic data as possible in the discovery
 186 data^{5,23,24}. The GWAS data is typically then processed by PRS methods that will
 187 adjust the SNP effect size using a set of hyper-parameters. Individual-level data of an
 188 independent fine-tuning sample is used to fine-tune the hyper-parameters across
 189 PRS methods and the combination of the fine-tuned PRS. The resulting PRS is
 190 expected to perform the best in samples of matched ancestry with the fine-tuning
 191 sample.
 192

193 The current approach, as shown in the left panel of Figure 1, is to use the multi-
194 GWAS PRS fine-tuned in the matched sample or the closest approximation when the
195 matched sample is unavailable. The pipeline of adjusting SNP effect sizes and
196 combining information from different GWAS varies widely. Without loss of generality,
197 we built the following pipeline as a representation of the current conventional method:
198 we first adjusted the SNP effect size of each of the summary statistical GWAS
199 datasets by a Bayesian method and then chose the most predictive PRS from all the
200 PRS generated under different hyper-parameters. For simulated GWAS data, we
201 used PRS-CS²⁵ to adjust the SNP effect size and LDpred2²⁶ for real GWAS. Then
202 we used the fine-tuning data to first select the most predictive PRS based on each
203 GWAS and then to train the linear combination of the most predictive single-GWAS
204 PRS with a linear regression model. The final PRS model generated from each of the
205 fine-tuning datasets is a linear combination of PRS. For the empiric data set, the PRS
206 were fine-tuned controlling for the following covariates: top 20 PCA, sex, and age.
207 We used AFR, EAS, EUR, SAS, AMR, and admixed samples to fine-tune the PRS. A
208 more detailed description of generating PRS weight from the one fine-tuning data
209 was given in Supplementary method section entitled 'Methodological Details of PRS
210 Construction Using a Single Fine-tuning Dataset'.
211

212 Simulated data results

213 Summary-level GWAS used as discovery data were generated based on simulated
214 genotype of AFR, EAS, EUR, and SAS population based on 1000 Genomes²⁷
215 reference as described in the previous publication provided by Zhang et al⁶. Fine-
216 tuning and testing samples were simulated based on UKBB genotype data. From
217 each ancestry group of AFR, EAS, EUR, SAS, and other (OTH) for admixed
218 individuals whose PCA information was not matched with any of the five ancestries
219 by 1000 Genome reference definition, 1.3k individuals were used as the training fine-
220 tuning datasets (See supplementary method section entitled 'Generating data for
221 simulation analysis'). The phenotype of discovery, fine-tuning, and testing data were
222 generated using the same pipeline and parameters: the phenotypes of 100, 300,
223 1,000, or 10,000 causal SNPs and heritability = 0.6 were simulated. Scenarios of
224 shared causal SNP with effect size constant across different ancestries and shared
225 causal SNP with effect size varying across population are both simulated. We used
226 up to 100,000 simulated individuals from AFR, EAS, EUR, and SAS to generate the
227 discovery summary statistic GWAS dataset with PLINK2²⁸ and left the remaining
228 samples out for other downstream analyses.

229
230 We primarily focused on the PRS performance in the admixed testing cohort.
231 DiscoDivas, which is based on PRS fine-tuned in AFR, EAS, EUR, and SAS, was
232 compared with the conventional PRS fine-tuned in the matched admixed fine-tuning
233 sample in scenarios of different causal SNP numbers, different discovery GWAS
234 sample sizes, and different causal SNP distribution across ancestry (See Figure 2)
235



236
237
238
239
240
241
242
243
244

Figure 2 Relative R^2 increase of DiscoDivas over the conventional PRS fine-tuned in a matched sample when tested in admixed individuals. The x-axis shows the simulated number of causal SNPs. The horizontal bar shows the mean relative R^2 increase and the color of the horizontal bar indicates the p -value of the paired t-test of DiscoDivas PRS R^2 and conventional PRS R^2 , with cyan being p -value<0.0005, dark blue being p -value<0.05 and grey being p -value>0.05. In panels a, b, and c, the causal SNP effect sizes are constant across different populations. The annotation texts on the top of each panel shows the sample size of discovery GWAS of different populations and the distribution of causal SNP effect sizes.

245

246 Although the comparison between DiscoDivas and the conventional method of fine-tuning PRS with matched ancestry sample in a single test iteration usually showed no statistical significance due to the small numeric differences, the paired t-test of DiscoDivas R^2 and the conventional PRS R^2 over the 20 iterations better clarified significant differences. When effect sizes of causal SNPs were held constant across different ancestries (Figure 2 panel a, b, and c), the PRS generated by DiscoDivas had comparable accuracy with the PRS fine-tuned using matched data. We noticed that when the sample size of non-European discovery GWAS dropped and the dataset was relatively more Eurocentric, the advantage of DiscoDivas became less statistically significant. In Figure 2 panel d, we compared DiscoDivas and the conventional PRS method of fine-tuning the PRS with matched ancestry in the scenario where causal SNPs were shared across all populations, but the effect sizes varied linearly in the PCA space. The advantage of DiscoDivas over conventional PRS method was more obvious in this scenario than when the effect sizes were constant across populations (Figure 2 panel a and d), presumably because personalized PRS combination with DiscoDivas better captured the changing effect sizes for the admixed testing sample. In all the scenarios tested, the advantage of DiscoDivas was least statistically significant when the number of causal SNPs was 10,000 but still significant when the number of causal SNPs was 1,000. Notably, the accuracy of both DiscoDivas and the conventional PRS method was the lowest when the number of causal SNPs was 10,000 (Supplementary Figure 1), indicating that the difference of the two PRS methods became less obvious when the input data became increasingly underpowered.

269

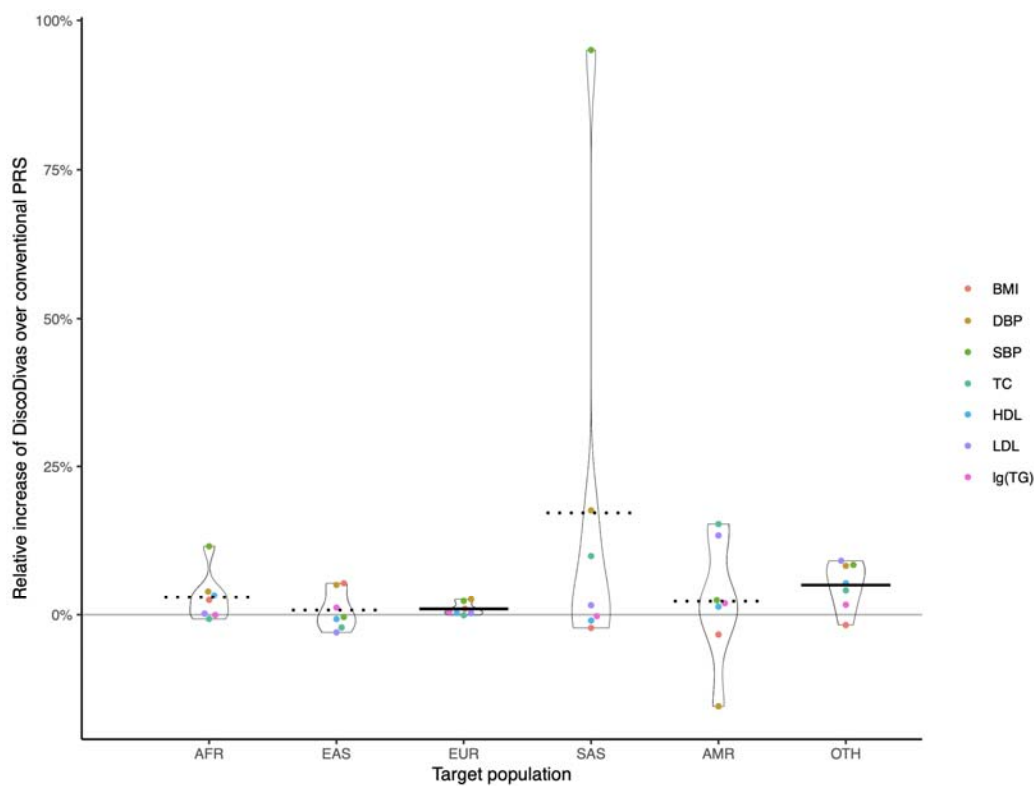
270 When predicting the individuals that are usually classified as single ancestries, i.e. 271 AFR, EAS, EUR, and SAS, DiscoDivas showed no statistically significant difference or a slight advantage over the conventional PRS method (Supplementary Figure 2). 272 When predicting AMR individuals, we used admixed fine-tuning data (OTH) to fine-tune the conventional PRS due to the small sample size of the AMR dataset. The 273 PRS performance when testing in the AMR dataset was similar as in admixed data 274 but the statistical significance was weaker, potentially due to the small sample size 275 276

277 and the high heterogeneity of the AMR dataset. In general, DiscoDivas showed its
278 clearest advantage over the conventional method of fine-tuning PRS with matched
279 PRS when the testing data and the fine-tuning data for the conventional method were
280 of different ancestries.
281
282

283 Biobank data results

284 We downloaded publicly available summary statistical data of body-mass index (BMI),
285 high-density lipoprotein cholesterol (HDL), low-density lipoprotein cholesterol (LDL),
286 total cholesterol (TC), triglycerides (TG), systolic blood pressure (SBP), diastolic
287 blood pressure (DBP), coronary artery disease (CAD), and diabetes mellitus (DM2)
288 and adjusted the SNP effect size using LDpred2 as described previously⁵.
289

290 For the quantitative traits, we used the fine-tuning samples of AFR, EAS, EUR, SAS,
291 and admixed (OTH) ancestry to fine-tune the model. The remaining UKBB samples
292 were used as the testing data. The results for empiric quantitative trait data were
293 highly aligned with the simulation results (Figure 4): DiscoDivas showed a robust
294 advantage over the conventional PRS method of fine-tuning PRS with matched or
295 similar ancestry samples when compared across the 7 traits in the admixed testing
296 dataset. When predicting AFR, EAS, EUR, and SAS, DiscoDivas and the
297 conventional PRS method had similar performance. The results of both methods in
298 AMR testing dataset had large deviations due to the small sample size and greater
299 genetic heterogeneity of the AMR data.
300
301



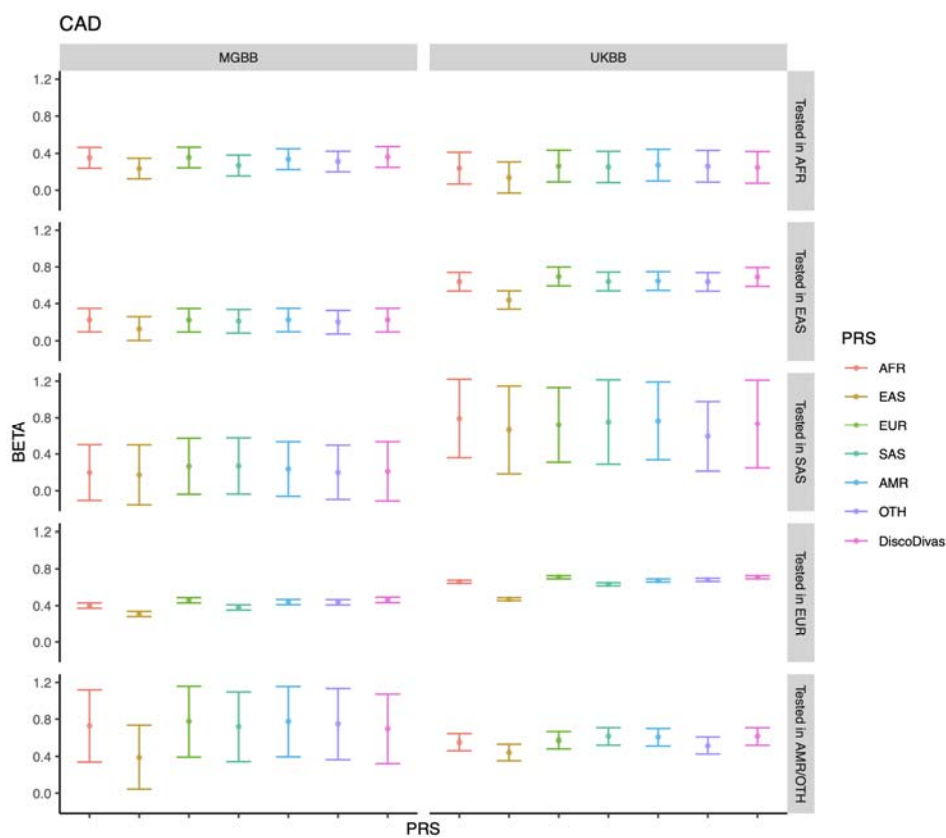
302
303 **Figure 3 Relative R^2 increase of DiscoDivas over the conventional PRS fine-tuned in a matched**
304 **sample.** The x-axis shows the population in which the PRS was tested. We used OTH as the fine-tuning

305 dataset for the test in both OTH and AMR due to the absence of matched AMR training data. The
 306 horizontal bar shows the mean of relative increase, and the line-type of the bar indicates the p -value of
 307 paired t-test of DiscoDivas PRS R^2 and conventional PRS R^2 , with the solid bar being p -value <0.05 and
 308 dotted bar being p -value >0.05 .

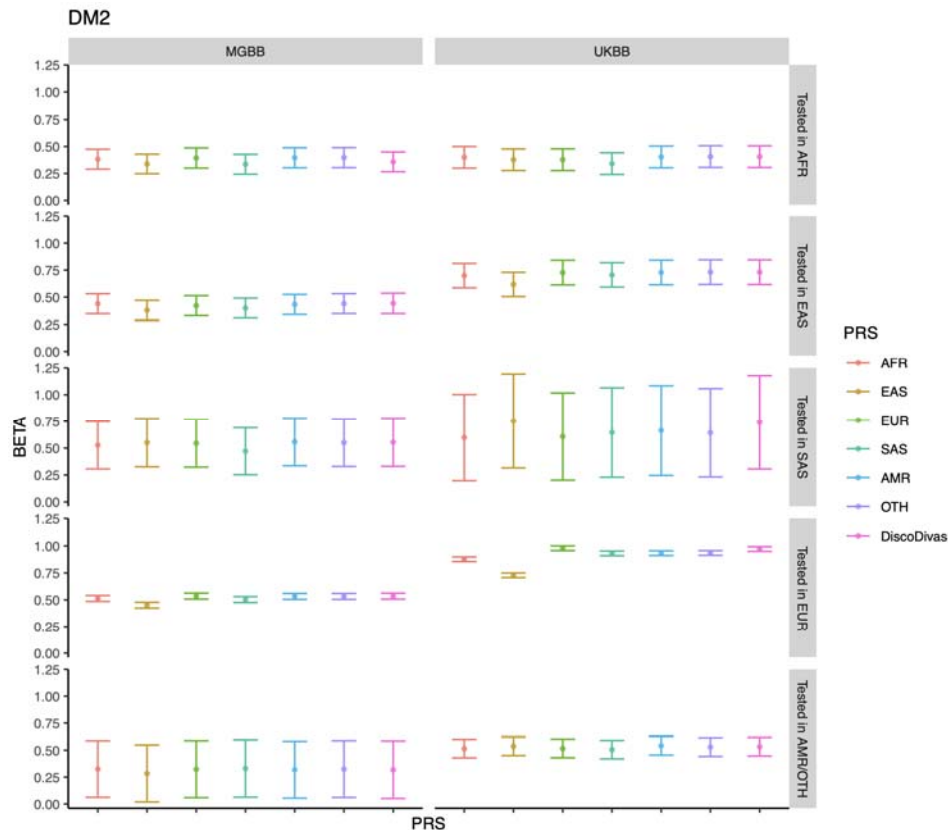
309 For the binary traits coronary artery disease (CAD) and type 2 diabetes (DM2)
 310 (Figure 4), we used the AFR, EAS, EUR, SAS, AMR, and OTH (i.e., unclassified)
 311 samples from AoU as the fine-tuning data and tested in AFR, EAS, EUR, SAS, and
 312 OTH individuals in UKBB and AFR, EAS, EUR, SAS, and AMR individuals in MGBB.
 313 The DiscoDivas PRS were based on the PRS fine-tuned in AFR, EAS, EUR, and
 314 SAS and used the default assumption that the PRS fine-tuned from all the samples
 315 were of similar quality even though the sample sizes of both discovery GWAS and
 316 the fine-tuning samples were not balanced across different ancestries. AMR in UKBB
 317 was excluded because of the small sample size (N=669).

318
 319 The PRS fine-tuned in different single samples and the DiscoDivas PRS had similar
 320 performances. It also appeared that some of the fine-tuning sample could be
 321 underpowered: generally, we expect the PRS fine-tuned in the matched sample to
 322 perform the best in the testing samples, but PRS fine-tuned in larger fine-tuning data
 323 performed better than PRS fine-tuned in smaller fine-tuning data in general. For
 324 example, the PRS fine-tuned in EAS AoU data performed worse than other PRS in
 325 both MGBB and UKBB EAS data and had low accuracy in other testing data as well;
 326 the CAD PRS fine-tuned in EUR performed better than all the other PRS in all the
 327 testing data and the effective sample size of EUR CAD fine-tuning data was much
 328 larger than all the other fine-tuning data.

329
 330



331



332
 333 **Figure 4 PRS performance for coronary artery disease (CAD) and type 2 diabetes (DM2) tested in**
 334 **UKBB and MGBB.** The plot shows OR per SD with the error bar showing 95% CI. The sub-panels show
 335 that population of the testing sample and the different colors show the method for generating the PRS,
 336 either fine-tuning in a single sample or combining the PRS using DiscoDivas.

337

338 Discussion

339 We propose a new method, DiscoDivas, to interpolate the PRS for diverse, especially
 340 admixed, ancestries with a generalized framework that does not requiring binning
 341 into discrete ancestries. Our results shows that the accuracy of DiscoDivas was
 342 comparable to or greater than the conventional method, i.e. fine-tuning using the
 343 matched population sample when available. In addition, when generating PRS for a
 344 wide range of ancestries, DiscoDivas did not require shifting from several sets of
 345 PRS weights fine-tuned in discrete samples while remaining matched with the
 346 ancestry information. Our method provides a new solution to generate PRS for
 347 underrepresented, generally admixed, populations and as well as generate a
 348 harmonized PRS model across different ancestries.

349

350 The performance of our method depends on the quality of both the discovery GWAS
 351 data and the fine-tuning data. As shown in the simulation test, discovery GWAS
 352 datasets that represent diverse ancestries with sufficient sample size will increase
 353 the accuracy of interpolated PRS generated by DiscoDivas. On the contrary,
 354 Eurocentric and underpowered discovery GWAS datasets would limit the advantage
 355 of DiscoDivas over the conventional PRS method. This might partly explain the
 356 limited advantage of DiscoDivas when predicting binary traits: the discovery GWAS
 357 datasets were highly Eurocentric and the GWAS, especially the non-European

358 cohorts, could be more underpowered than quantitative trait GWAS. Furthermore, the
359 PRS fine-tuned in fine-tuning datasets of insufficient sample size will be overfitted
360 and cannot be used to fairly evaluate the performance of either the conventional PRS
361 method or DiscoDivas. We aimed to address this issue by only using traits that 1)
362 had effective sample sizes larger than 200 in all the fine-tuning samples, and 2) had
363 high-quality phenotyping data in both the fine-tuning datasets and the testing
364 datasets. However, Asian populations were largely under-represented in the current
365 public biobanks: the effective sample size of many binary traits in EAS or SAS can be
366 as small as <200 even in AoU, the most diverse and large-scale largely publicly-
367 available biobank we had access to. This limited our choice for binary traits to only
368 CAD and DM2. One additional limitation of our method is that DiscoDivas does not
369 consider the local ancestry information, which improve PRS predictions in various
370 research^{24,29,30}, especially PRS prediction of newly admixed populations³¹.

371
372 Our research underscores the notion that non-European populations, both admixed
373 and single-ancestry populations, remain largely under-represented in the existing
374 genetic data. Furthermore, some potential extensions of our method will not become
375 possible until we collect more diverse and larger datasets. First, our method has not
376 been designed nor tested for extrapolating data, e.g. generating PRS for continental
377 African samples based on African American, European, and Asian samples. Even
378 though it is mathematically plausible to alter our method to extrapolate the PRS, we
379 lack data such as continental African samples to test the method. Secondly, we
380 currently only consider the assumption that the most informative genome-wide PRS
381 weight shifts linearly in the PCA space. Although more complicated PRS interpolation,
382 e.g. interpolation guided by local ancestry information^{24,29,30}, pathway-specific^{32,33}
383 and annotation-guided³⁴ PRS weights and polynomial interpolation^{35,36}, can possibly
384 further improve the PRS accuracy, training such complicated models would require
385 collecting much larger and more diverse datasets than the existing data. Finally,
386 additional biological insights could be revealed by interpolating PRS if genetic data of
387 all the involved diverse ancestries are of sufficient power. In this case, the differences
388 between interpolated PRS and the PRS trained using the matched ancestry would
389 indicate the population- or sample- specific factors absent in the interpolation model,
390 e.g. population-specific genetic variance³⁷, complicated population stratification
391 involving confounding factors^{38,39}, sample/ancestry-specific modifiers like local
392 adaptation³⁸, gene x environment interactions⁴⁰ or other factors that contribute to the
393 genetic variant frequency or effect size in these samples/ ancestries.

394
395 In conclusion, our method provides a new option to treat the ancestry information as
396 a continuous variable and interpolate a harmonized PRS for diverse ancestries.
397 Notably, although our method was developed primarily to calculate PRS when the
398 matched fine-tuning datasets were unavailable, our research showed that
399 successfully interpolating PRS required sufficient input data and highlighted the need
400 to collect genetic data for underrepresented populations. We believe that more
401 diverse and larger data collected in the coming future will enable the development of
402 new methods of interpolating PRS and the elucidation of the genetic basis of
403 complex traits.
404

405 **Methods**

406 Calculation of 1000 Genomes–based PCA and Euclidean 407 distance

408 We use 1000 Genomes as the reference panel for PCA calculation. The PCA should
409 be based on SNPs that are constantly included in as many samples as possible to
410 enable the use of wide-ranging discovery GWAS and fine-tuning datasets. We
411 started with the Hapmap3 SNPs for this set of SNPs, which has been widely used as
412 a subset of SNPs that approximates the feature of genome-wide common SNPs in
413 many recent studies that involve multi-ancestry prediction^{6,25,26,41}. We further filtered
414 for the SNPs likely to be frequently genotyped or imputed with relatively high quality
415 by most samples based on the 1000 Genome data: Hapmap3 SNPs were first
416 extracted from the five super-populations, Africans (AFR), Admixed Americans
417 (AMR), East Asians (EAS), Europeans (EUR) and South Asians (SAS) of the 1000
418 Genomes. Secondly, SNPs described as the following were excluded: 1) of minor
419 allele frequency lower than 1% in any of the super-population, 2) of minor allele
420 frequency lower than 5% in the combined 1000 Genomes data, and 3) in the long-
421 range LD region (25Mb – 35Mb by hg19 assembly on chromosome 6 and 7Mb –
422 13Mb on chromosome 8). To calculating the PCA loading, the QC'ed SNPs of the
423 five super-populations were merged then pruned using the PLINK2 function “indep-
424 pairwise” with the parameter “200 100 0.1” - namely the pruning was performed using
425 window size = 200kb, step size = 100, and phased-hardcall-r²= 0.1. The principal
426 components and the SNP loadings are calculated using PLINK2 function “pca” with
427 the parameter “allele-wts” based on the pruned SNPs.

428
429 Based on the protocol suggested on the PLINK2 website ([https://www.cog-
430 genomics.org/plink/2.0/score#pca_project](https://www.cog-genomics.org/plink/2.0/score#pca_project)), we projected samples for fine-tuning and
431 PRS testing into the PCA space as describe above by calculation the linear score, i.e.
432 the sum of alternative alleles weighted by the SNP effect size, using the PLINK2
433 function “score” with the SNP loadings as effect size. The original online protocol
434 suggested linear score should be first scaled to standard variation and then rescaled
435 by multiplying the square root of eigenvalue. However, the actual standard deviation
436 of a sample in the same PCA space varies with the homogeneity and the ancestry of
437 the sample. Forcing the PCA of all the samples to have the same standard deviation
438 will cause inconsistent scaling when the samples can be of different ancestries.
439 Therefore, we directly calculated the PCA from sum basic linear score based on the
440 SNP loadings as generated above without any further scaling. The PCA in this study
441 was the sum basic linear score calculated using the PLINK2 function “score” with the
442 parameter “cols+=scoresums”. For large samples whose genotype data were divided
443 into per-chromosome files, the same commands were used to calculate per-
444 chromosome score and the genome-wide score was the sum of the score of all the
445 autosomes.

446
447 In DiscoDivas' default setting, the genetic distance between two individuals is defined
448 as the Euclidian distance between the PCA of the two individuals. When the genetic
449 distance calculation involves a sample, we use the median point to present the whole
450 sample.

451
452 We also explored the relationship between number of PCs included in the calculation

453 and the Euclidean distance calculated (Supplementary Figure 9) and the distance
454 calculated converged when the number of PCs was larger than 6 in our tests. In our
455 analysis we use the top 10 PCs to calculate the PCs.
456

457 Genetic ancestry reference

458 We noticed that the protocol of generating top PCs for ancestry references varied in
459 previous publications. In our pilot test (see supplementary results section entitled
460 'Pilot test of generating PCA based on less QC'ed SNPs'), we compared the ancestry
461 reference based on Hapmap3 SNP without any QC and found the result to be highly
462 correlated. We used the same set of PCs based on QC'ed SNP as described in
463 section 'Calculation of 1000 Genomes-based PCA and Euclidean distance' for both
464 genetic ancestry reference and Euclidean distance calculation for data consistency.
465

466 Random forest model of 100 trees was trained based on the 1000 Genome data. The
467 out-of-bag estimate of error rate stabilize at the level of 0.28% after the number of
468 PCs passed 5. We used the model using the top 6 PCs to infer the genetic ancestry
469 of UK Biobank individuals and the Mass General Brigham Biobank individuals. The
470 genetic ancestry of an individual was assigned to any of the five ancestries
471 represented in the 1000 Genomes reference data, i.e. AFR, AMR, EAS, EUR and
472 SAS, if the highest probability of an individual belonging to that ancestry passed a
473 threshold. If none of the ancestries had a probability above the threshold, the
474 individuals were assigned as other (OTH), which indicated that the individual was of
475 admixed ancestries. With the consideration of the sample size and confirmed by
476 visual inspection, the threshold of probability for UK Biobank and the Mass General
477 Brigham Biobank was 0.9 and 0.8 respectively.
478

479 Data

480 UK Biobank

481 The UK Biobank (UKBB) is a volunteer sample of approximately 500,000 adults aged
482 40-69 upon enrollment living in the United Kingdom recruited since 2006⁴². UKBB
483 data used in this research were first QC'ed with the following process: Remove the
484 individuals meeting the criteria that indicate low genotype quality or contamination: 1)
485 have missing genotype rate larger than 0.02; 2) have genotype-phenotype sex
486 discordance; 3) are identified as having excess heterozygosity and missing rates; 4)
487 are identified as putatively carrying sex chromosome configurations that are not
488 either XX or XY; 5) appeared to have unreasonably large numbers of relatives. From
489 the remaining samples, individuals from a group of multiple individuals that are closer
490 than 3rd-degree relatives were retained. 415,402 individuals were left after the QC.
491 390,037 were self-identified as EUR, 7,039 AFR, 8,652 non-Chinese Asian (ASN),
492 1430 Chinese (CHN) and 6572 unknown or not answered, and 1672 as admixed
493 (MIX). The genetic ancestry referred from PC was largely correlated with the self-
494 reported race, with 385,038 EUR, 7,450 AFR, 8,298 SAS, 2,163 EAS, 669 AMR and
495 11,784 other (OTH) or admixed.
496

497 In the PRS test, UKBB samples were grouped by their genetic ancestry (see section
498 'Genetic ancestry reference'). The fine-tuning datasets for the single-ancestry
499 populations (AFR, EAS, EUR and SAS) were based on 1.3k randomly selected
500 samples whose self-report ancestry matched with their genetic ancestry and the

501 probability of random forest = 1. The fine-tuning dataset for admixed ancestry (OTH)
502 is 1.3k randomly selected samples of individuals of OTH genetic ancestry (see
503 Supplementary Figure 3). AMR didn't have its corresponding fine-tuning dataset due
504 to its small sample size and we used OTH fine-tuning datasets as a proxy since the
505 two genetic ancestries had similar PCA. The remaining individuals of UKBB were
506 used as testing data.

507

508 The quantitative trait of the UKBB samples was the measurement collected after the
509 participants enrolled. The lipid trait measurement was adjusted for cholesterol-
510 lowering medication by dividing TC by 0.8 and LDL by 0.7 as before⁴³. Cases of
511 coronary artery diseases (CAD) are defined using the definition described
512 previously²⁴; Cases of diabetes are defined as ever report the following code: E10X,
513 E11X, E12X, E13X, and E14X where X can be any integer between 0 to 9 in the
514 ICD10 diagnosis code.

515

516 UKBB participants provided consent in accordance with the primary IRB protocol,
517 and the Massachusetts General Hospital IRB approved the present secondary data
518 analysis of the UKBB data under UKBB application 7089.

519

520 **Mass General Brigham Biobank**

521 The Mass General Brigham Biobank (MGBB) is a volunteer sample of approximately
522 142,000 participants receiving medical care in the Mass General Brigham health care
523 system recruited starting 2010. 53,306 MGBB participants underwent genotyping via
524 Illumina Global Screening Array (Illumina, CA). MGBB genotype data was quality
525 controlled, imputed and assigned one of the populations AFR, AMR, EAS, EUR, SAS
526 using K-nearest neighbor model as described previously⁴⁴. The phenotype data of
527 CAD and diabetes are drawn from PheCodes based on International Classification of
528 Diseases codes, Ninth (ICD9)110 and Tenth (ICD10) revisions, from the EHR as
529 described previously³². MGBB participants provided consent in accordance with the
530 primary IRB protocol, and the Massachusetts General Hospital IRB approved the
531 present secondary data analysis.

532

533 **All of Us Research Program**

534 The *All of Us* (AoU) Research Program is a volunteer sample of more than one
535 million United States residents recruited starting 2016. AoU aims to engage
536 communities previously underrepresented in biomedical research in the United
537 States and beyond⁴⁵. In the present analysis, genetic data from the v7 245,394
538 participants who were genotyped using short read whole genome sequencing
539 (srWGS) data. Hapmap3 SNPs were extracted for the callset with the threshold of
540 (AF) > 1% or population-specific allele count (AC) > 100. Related individuals were
541 pruned according to the information provided by AoU. Due to the inclusive data
542 collection, we didn't excluded individuals whose self-report gender were different with
543 their assigned sex at birth and used the combination of self-report gender and
544 assigned sex as one of the covariates. The predicted ancestry information was
545 provided by AoU⁴⁶. The phenotypes were defined as described in previous research
546 by Buu *et al*⁴⁷.

547

548 **Simulated data**

549 The simulated GWAS summary statistics were based on simulated genotype data
550 based on 1000 Genomes reference⁶. Only Hapmap3 SNPs were included in the
551 simulation. Causal SNPs were randomly selected from the Hapmap3 SNPs and
552 simulated per allele effect size following normal distribution. The ladder of causal

553 SNP number was 100, 1000, 3000, 10000 and the heritability in each of the
554 population was 0.6. The causal SNP effect size was simulated as either constant
555 across populations or varying linearly in the PCA space.
556 The phenotype is the sum of genetic burden and non-genetic factor:

$$phenotype_i = \sum \beta_j x_{j,i} + E_i$$

557 where the $phenotype_i$ and E_i were the phenotype and non-genetic factor of individual
558 i ; β_j was the effect size of causal SNP j , and $x_{j,i}$ was the number of risk alleles of
559 individual i in SNP j .

560
561 We used the PLINK2²⁸ to calculate the genetic burden based on the simulated causal
562 SNPs and effect size and used R to simulate the non-genetic factors, scale the
563 genetic burden and non-genetic factor, and generate a phenotype of heritability set to
564 be 0.6. We used up to 100k individuals per population to generate the summary
565 statistical GWAS as the discovery data for the PRS test. The rest simulated data
566 were left out for the fine-tuning and testing datasets. The summary statistics GWAS
567 were generated based on the simulated genotype data and phenotype data using the
568 '--glm' function of PLINK2.

569
570 In addition to the completely simulated data, we generated more realistic fine-tuning
571 and testing datasets of a wider ancestry range by using the QC'ed genotype data
572 from UKBB described in the section 'Biobank data.' We simulated the genetic burden,
573 non-genetic factor, and phenotype based on the real-life UKBB genotype data with
574 the same pipeline and parameters. A more detailed description of simulating the data
575 were given in section 'Generating data for simulation analysis' in the supplementary
576 text.
577

578 Acknowledgement

579 We thank the participants and staff of the UK Biobank (application 7089), Mass
580 General Brigham Biobank, and *All of Us* Research Program. We thank Ying Wang,
581 Paul O'Reilly, Raymond Walters for helpful discussion and advice.
582

583 Contributions

584 Y.R. and P.N. designed the project; Y.R. developed the statistical methods and
585 programmed the code for DiscoDivas. A.P. curated the summary statistical GWAS.
586 R.B, S.K, L.H, B.T, and W.H participated in application for the access to the Biobank
587 data and the data curation. Y.R and R.B performed the data analysis. R.B, B.T, H.Z,
588 and N.C contributed to the method development. Y.R. and P.N wrote the manuscript.
589 A.P. and N.C. provided critical revision for the manuscript. All the authors reviewed
590 and approved the final version of the manuscript.
591

592 Data Availability

593 The access to biobank data (UK Biobank, Mass General Brigham Biobank, and All of

594 US Research Program) were gained upon application. The simulated genotype data
595 based on 1000 Genomes were downloaded from
596 <https://dataverse.harvard.edu/dataset.xhtml?persistentId=doi:10.7910/DVN/COXHAP>
597 ;The resource of summary statistics GWAS data used to generate PRS were given in
598 the supplementary file. The 1000 Genome raw reference genotype data were
599 downloaded from <https://cncr.nl/research/magma/>.
600

601 Code Availability

602 The scripts of running DiscoDivas and other supporting files can be found at
603 <https://github.com/YunfengRuan/DiscoDivas>; PRS-CS:
604 <https://github.com/getian107/PRScs>; LDpred2:
605 <https://privefl.github.io/bigsnpr/articles/LDpred2>; PLINK2: [https://www.cog-
606 genomics.org/plink/2.0/](https://www.cog-genomics.org/plink/2.0/).
607

608 Reference

- 609 1. Martin, A. R. *et al.* Clinical use of current polygenic risk scores may
610 exacerbate health disparities. *Nat Genet* **51**, 584–591 (2019).
- 611 2. Miao, J. *et al.* Quantifying portable genetic effects and improving cross-
612 ancestry genetic prediction with GWAS summary statistics. *Nat Commun* **14**,
613 832 (2023).
- 614 3. Ruan, Y. *et al.* Improving polygenic prediction in ancestrally diverse
615 populations. *Nat Genet* **54**, 573–580 (2022).
- 616 4. Jin, J. *et al.* MUSSEL: Enhanced Bayesian Polygenic Risk Prediction
617 Leveraging Information across Multiple Ancestry Groups. *bioRxiv*
618 2023.04.12.536510 (2023) doi:10.1101/2023.04.12.536510.
- 619 5. Patel, A. P. *et al.* A multi-ancestry polygenic risk score improves risk prediction
620 for coronary artery disease. *Nat Med* **29**, 1793–1803 (2023).
- 621 6. Zhang, H. *et al.* A new method for multiancestry polygenic prediction improves
622 performance across diverse populations. *Nat Genet* **55**, 1757–1768 (2023).
- 623 7. Ding, Y. *et al.* Polygenic scoring accuracy varies across the genetic ancestry
624 continuum. *Nature* **618**, 774–781 (2023).
- 625 8. Landry, L. G., Ali, N., Williams, D. R., Rehm, H. L. & Bonham, V. L. Lack Of
626 Diversity In Genomic Databases Is A Barrier To Translating Precision
627 Medicine Research Into Practice. *Health Aff* **37**, 780–785 (2018).
- 628 9. The All of Us Research Program Genomics Investigators. Genomic data in the
629 All of Us Research Program. *Nature* **627**, 340–346 (2024).
- 630 10. Fatumo, S. *et al.* Polygenic risk scores for disease risk prediction in Africa:
631 current challenges and future directions. *Genome Medicine* vol. 15 Preprint at
632 <https://doi.org/10.1186/s13073-023-01245-9> (2023).
- 633 11. Dokuru, D. R., Horwitz, T. B., Freis, S. M., Stallings, M. C. & Ehringer, M. A.
634 South Asia: The Missing Diverse in Diversity. *Behav Genet* **54**, 51–62 (2024).
- 635 12. Stefflova, K. *et al.* Dissecting the Within-Africa ancestry of populations of
636 African descent in the Americas. *PLoS One* **6**, (2011).
- 637 13. Harlemon, M. *et al.* A custom genotyping array reveals population-level
638 heterogeneity for the genetic risks of prostate cancer and other cancers in
639 Africa. *Cancer Res* **80**, 2956–2966 (2020).

- 640 14. Anagnostou, P. *et al.* Inter-individual genomic heterogeneity within European
641 population isolates. *PLoS One* **14**, (2019).
- 642 15. Pan, Z. & Xu, S. Population genomics of East Asian ethnic groups. *Hereditas*
643 vol. 157 Preprint at <https://doi.org/10.1186/s41065-020-00162-w> (2020).
- 644 16. Khera, A. V *et al.* Whole-Genome Sequencing to Characterize Monogenic and
645 Polygenic Contributions in Patients Hospitalized With Early-Onset Myocardial
646 Infarction. *Circulation* **139**, 1593–1602 (2019).
- 647 17. Duncan, L. *et al.* Analysis of polygenic risk score usage and performance in
648 diverse human populations. *Nat Commun* **10**, 3328 (2019).
- 649 18. Wang, M. *et al.* Validation of a Genome-Wide Polygenic Score for Coronary
650 Artery Disease in South Asians. *J Am Coll Cardiol* **76**, 703–714 (2020).
- 651 19. Ge, T. *et al.* Development and validation of a trans-ancestry polygenic risk
652 score for type 2 diabetes in diverse populations. *Genome Med* **14**, 70 (2022).
- 653 20. O'Sullivan, J. W. *et al.* Polygenic Risk Scores for Cardiovascular Disease: A
654 Scientific Statement From the American Heart Association. *Circulation* vol. 146
655 E93–E118 Preprint at <https://doi.org/10.1161/CIR.0000000000001077> (2022).
- 656 21. Lewis, C. M. & Vassos, E. Polygenic risk scores: From research tools to
657 clinical instruments. *Genome Medicine* vol. 12 Preprint at
658 <https://doi.org/10.1186/s13073-020-00742-5> (2020).
- 659 22. Xiang, R. *et al.* Recent advances in polygenic scores: translation, equitability,
660 methods and FAIR tools. *Genome Medicine* vol. 16 Preprint at
661 <https://doi.org/10.1186/s13073-024-01304-9> (2024).
- 662 23. Truong, B. *et al.* Integrative polygenic risk score improves the prediction
663 accuracy of complex traits and diseases. *Cell Genomics* **4**, (2024).
- 664 24. Wang, Y. *et al.* Polygenic prediction across populations is influenced by
665 ancestry, genetic architecture, and methodology. *Cell Genomics* **3**, (2023).
- 666 25. Ge, T., Chen, C.-Y., Ni, Y., Feng, Y.-C. A. & Smoller, J. W. Polygenic
667 prediction via Bayesian regression and continuous shrinkage priors. *Nat*
668 *Commun* **10**, 1776 (2019).
- 669 26. Privé, F., Arbel, J. & Vilhjálmsón, B. J. LDpred2: better, faster, stronger.
670 *Bioinformatics* **36**, 5424–5431 (2021).
- 671 27. Auton, A. *et al.* A global reference for human genetic variation. *Nature* **526**,
672 68–74 (2015).
- 673 28. Chang, C. C. *et al.* Second-generation PLINK: Rising to the challenge of larger
674 and richer datasets. *Gigascience* **4**, (2015).
- 675 29. Atkinson, E. G. *et al.* Tractor uses local ancestry to enable the inclusion of
676 admixed individuals in GWAS and to boost power. *Nat Genet* **53**, 195–204
677 (2021).
- 678 30. Sun, Q. *et al.* Improving polygenic risk prediction in admixed populations by
679 explicitly modeling ancestral-differential effects via GAUDI. *Nat Commun* **15**,
680 (2024).
- 681 31. Marnetto, D. *et al.* Ancestry deconvolution and partial polygenic score can
682 improve susceptibility predictions in recently admixed individuals. *Nat*
683 *Commun* **11**, (2020).
- 684 32. Xu, Y. *et al.* Effect of Pathway-Specific Polygenic Risk Scores for Alzheimer's
685 Disease (AD) on Rate of Change in Cognitive Function and AD-Related
686 Biomarkers Among Asymptomatic Individuals. *Journal of Alzheimer's Disease*
687 **94**, 1587–1605 (2023).
- 688 33. Tubbs, J. D. *et al.* Pathway-Specific Polygenic Scores Improve Cross-Ancestry
689 Prediction of Psychosis and Clinical Outcomes. Preprint at
690 <https://doi.org/10.1101/2023.09.01.23294957> (2023).
- 691 34. Miao, J. *et al.* Quantifying portable genetic effects and improving cross-
692 ancestry genetic prediction with GWAS summary statistics. *Nat Commun* **14**,

- 693 (2023).
694 35. Kumar, R., Bhattacharya, S. & Murmu, G. Exploring Optimality of Piecewise
695 Polynomial Interpolation Functions for Lung Field Modeling in 2D Chest X-Ray
696 Images. *Front Phys* **9**, (2021).
697 36. Womersley, R. S. & Sloan, I. H. *How Good Can Polynomial Interpolation on*
698 *the Sphere Be? Advances in Computational Mathematics* vol. 14 (2001).
699 37. Choudhury, A. *et al.* Population-specific common SNPs reflect demographic
700 histories and highlight regions of genomic plasticity with functional relevance.
701 *BMC Genomics* **15**, (2014).
702 38. Rees, J. S., Castellano, S. & Andrés, A. M. The Genomics of Human Local
703 Adaptation. *Trends in Genetics* vol. 36 415–428 Preprint at
704 <https://doi.org/10.1016/j.tig.2020.03.006> (2020).
705 39. Mas-Sandoval, A., Mathieson, S. & Fumagalli, M. The genomic footprint of
706 social stratification in admixing American populations. **12**, 84429 (2023).
707 40. Patel, R. A. *et al.* Genetic interactions drive heterogeneity in causal variant
708 effect sizes for gene expression and complex traits. *Am J Hum Genet* **109**,
709 1286–1297 (2022).
710 41. Yengo, L. *et al.* A saturated map of common genetic variants associated with
711 human height. *Nature* **610**, 704–712 (2022).
712 42. Bycroft, C. *et al.* The UK Biobank resource with deep phenotyping and
713 genomic data. *Nature* **562**, 203–209 (2018).
714 43. Graham, S. E. *et al.* The power of genetic diversity in genome-wide
715 association studies of lipids. *Nature* **600**, 675–679 (2021).
716 44. Koyama, S. *et al.* Decoding Genetics, Ancestry, and Geospatial Context for
717 Precision Health. *medRxiv* (2023) doi:10.1101/2023.10.24.23297096.
718 45. Kathiresan, N. *et al.* Representation of Race and Ethnicity in the
719 Contemporary US Health Cohort All of Us Research Program. *JAMA Cardiol* **8**,
720 859–864 (2023).
721 46. Bick, A. G. *et al.* Inherited causes of clonal haematopoiesis in 97,691 whole
722 genomes. *Nature* **586**, 763–768 (2020).
723 47. Truong, B. *et al.* Integrative polygenic risk score improves the prediction
724 accuracy of complex traits and diseases. *medRxiv* (2023)
725 doi:10.1101/2023.02.21.23286110.
726